Strength of Materials, Vol. 40, No. 1, 2008

CORROSION FATIGUE BEHAVIOR OF EXTRUDED AZ80, AZ61, AND AM60 MAGNESIUM ALLOYS IN DISTILLED WATER

Y. Uematsu,[1,a] K. Tokaji,[1,b] and T. Ohashi[2]

UDC 539.4

Rotary bending fatigue tests were conducted in laboratory air and distilled water using three extruded magnesium (Mg) alloys AZ80, AZ61, and AM60 with different chemical compositions. In laboratory air, the fatigue strengths at high stress levels were similar in all alloys because cracks initiated at Al–Mg intermetallic compounds, whereas AZ80 with the largest Al content exhibited the highest fatigue strength at low stress levels, which was attributed to the crack initiation due to cyclic slip deformation in the matrix microstructure. In distilled water, fatigue strengths were considerably decreased due to the formation of corrosion pits in all alloys, and the difference of fatigue strength at low stress levels among the alloys disappeared, indicating that the addition of Al that improved the fatigue strength in laboratory air was detrimental to corrosion fatigue.

Keywords: fatigue, corrosion fatigue, magnesium alloy, crack initiation.

Introduction. Mg alloys have recently received considerable attention due to their excellent properties such as light weight, high specific strength and stiffness, etc. Wrought Mg alloys have superior mechanical properties to cast Mg alloys, but various fatigue properties should be evaluated in detail for their applications to load-bearing components [1]. Furthermore, it is well known that Mg alloys have poor corrosion resistance [2]. Therefore, understanding the corrosion fatigue behavior of Mg alloys is also very important [3]. In the present study, rotary bending fatigue tests have been performed in laboratory air and distilled water using three extruded Mg alloys AZ80, AZ61, and AM60 with different chemical compositions, where the Al and Zn contents are considerably different. The effect of chemical composition of Mg alloys on corrosion fatigue behavior was discussed.

Experimental Details. ***Materials and Specimen.*** The materials used are extruded AZ80, AZ61, and AM60 alloys. Their chemical compositions (in wt.%) and mechanical properties are listed in Tables 1 and 2, respectively. The tensile strength increases with increasing the Al content. The average grain sizes are 12, 17.9, and 8.7 μm for AZ80, AZ61, and AM60, respectively. Smooth fatigue specimens with a diameter of 8 mm and a gauge length of 10 mm were machined from the extruded materials. All specimens were sampled from the same lot extruded bars in order to avoid large scatter in $S-N$ data.

Procedures. Fatigue tests were performed using a 98 Nm capacity rotary bending fatigue testing machine operating at a frequency of 20 Hz in laboratory air. Corrosion fatigue tests were conducted using the same testing machine where distilled water was dropped onto the centre of gauge length by a metering pump whose flow rate was 140 ml/min.

Results and Discussion. ***Fatigue Behavior in Laboratory Air.*** *Fatigue Strength*. In the following Figures 1, 5 and 6, the test results in laboratory air and distilled water are shown by open and solid symbols, respectively. The $S-N$ diagram is revealed in Fig. 1. The fatigue strengths at high stress levels are similar in all alloys, indicating that chemical composition has little effect. However, the fatigue limits defined as the fatigue strengths at $N=10^7$ cycles are 80 MPa for AZ61 and AM60 and 100 MPa for AZ80. Therefore, the addition of Al can improve not only tensile strength but also fatigue limit.

[1]Gifu University, Gifu, Japan. [2]Brother Industries Ltd, Nagoya, Japan. / [a] yuematsu@gifu-u.ac.jp, [b] tokaji@gifu-u.ac.jp / Translated from Problemy Prochnosti, No. 1, pp. 141 – 145, January – February, 2008. Original article submitted June 28, 2007.

TABLE 1. Chemical Compositions of Materials (wt.%)

Material	Al	Zn	Mn	Ni	Cu	Fe	Si	Pb	Ca	Sn	Mg
AZ80	8.3	0.60	0.23	0.0010	0.0020	0.002	0.030	–	–	–	Balanced
AZ61	6.4	0.74	0.35	0.0012	0.0029	0.001	0.015	0.001	0.001	<0.001	ditto
AM60	6.0	0.02	0.32	0.0005	0.0030	0.003	0.030	–	–	–	ditto

TABLE 2. Mechanical Properties of Materials

Material	0.2% proof stress $\sigma_{0.2}$, MPa	Tensile strength σ_b, MPa	Elongation δ, %	Reduction of area Ψ, %
AZ80	196	273	14.6	13.1
AZ61	186	248	14.0	23.8
AM60	196	246	13.1	32.6

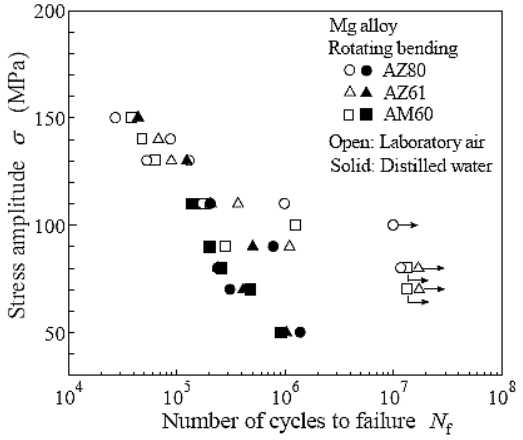

Fig. 1. $S-N$ diagram.

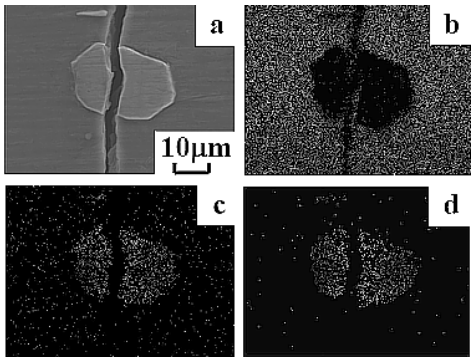

Fig. 2. EDX analysis results at crack initiation site in AM60 ($\sigma = 140$ MPa): (a) SEM image, (b) Mg, (c) Al, (d) Mn.

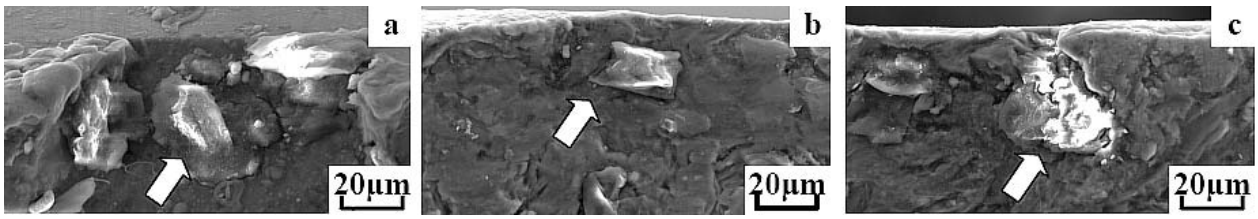

Fig. 3. SEM micrographs showing crack initiation site in laboratory air ($\sigma = 150$ MPa): (a) AZ80, (b) AZ61, (c) AM60.

Crack Initiation Behavior. Figure 2a indicates SEM micrograph of crack initiation site in AM60, where the stress level, σ, was 140 MPa. The crack is initiated due to the breakage of an inclusion. The results of EDX mapping analysis are also shown in the figure, which indicates that the inclusion mainly consists of aluminum and manganese, thus it was identified as Al–Mn-based intermetallic compound. Similar inclusions were also recognized in AZ80 and AZ61. The SEM micrographs of fracture surface near crack initiation site are revealed in Figs. 3 and 4 for high and low stress levels, respectively. Inclusions are recognized at the crack initiation site in all alloys as shown by arrow in Fig. 3 at high stress level ($\sigma = 150$ MPa), but not in Fig. 4 at low stress level ($\sigma = 110$ MPa). Inclusions were observed at the crack initiation sites in all alloys only when stress levels were higher than 130 MPa. Therefore, it is concluded that cracks are initiated from inclusion at high stress levels, while due to cyclic slip deformation in the matrix microstructure when stress levels were lower than 130 MPa as shown in Fig. 4.

Small Crack Growth Behavior. The surface crack length, $2c$, is represented in Fig. 5 as a function of cycle ratio, N/N_f (N_f is fatigue life). Cracks initiated at an early stage of fatigue life, indicating that fatigue life was

Fig. 4. SEM micrographs showing crack initiation site in laboratory air ($\sigma = 110$ MPa): (a) AZ80, (b) AZ61, (c) AM60.

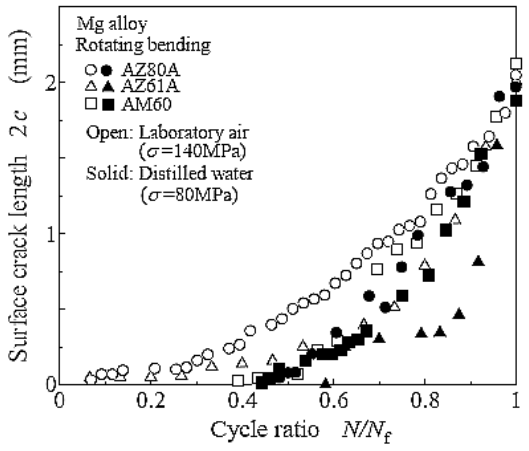

Fig. 5

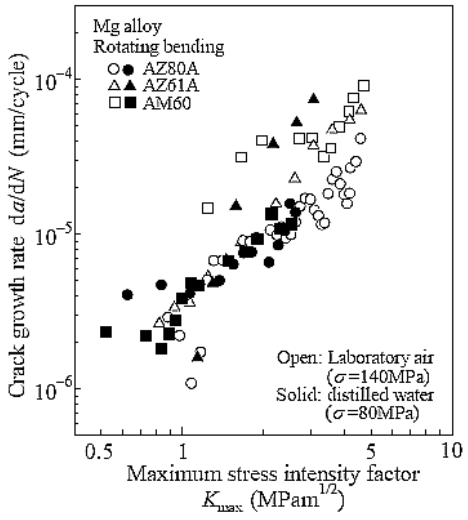

Fig. 6

Fig. 5. Relationship between surface crack length and cycle ratio.
Fig. 6. Relationship between crack growth rate and maximum stress intensity factor.

dominated mainly by small crack growth. Figure 6 shows the relationship between crack growth rate, da/dN, and maximum stress intensity factor, $K_{\max}$. The crack growth rates become slightly slower in the order of AM60, AZ61, and AZ80, revealing that the addition of Al can improve small crack growth resistance.

It is believed that crack initiation from inclusion at high stress levels results in the similar fatigue strength regardless of chemical composition, while when low stresses were applied, cracks initiated due to cyclic slip deformation. Therefore, AZ80 with the highest Al content and tensile strength has the highest fatigue limit.

Fatigue Behavior in Distilled Water. *Fatigue Strength*. The fatigue strength values at high stress levels in distilled water are similar to those in laboratory air, while fatigue fracture occurs even if stress levels are lower than the fatigue limit in laboratory air. The fatigue strength values of all alloys are nearly the same, thus AZ80 that exhibited the highest fatigue limit in laboratory air is most sensitive to the corrosive environment.

Crack Initiation Behavior. Figure 7 shows SEM micrographs of fracture surface near crack initiation site at a stress level of 50 MPa that is lower than the fatigue limit in laboratory air. The specimen was tilted about an angle of 45° in order to observe the specimen surface. It is clear that the specimen surface is covered by cracked corrosion product, and corrosion pit shown by allow is recognized at the crack initiation site. Figure 8 represents the specimen surfaces of AM60 tested at a stress level of 50 MPa in distilled water. In all alloys, the specimen surfaces are covered by corrosion product and many corrosion pits are formed as typically seen in Fig. 8. However, corrosion pits were not recognized on the specimen surface or the crack initiation site when higher stresses were applied, namely test period was short. Therefore, it can be concluded that corrosion pit is formed at low stress levels, where test period was long, and cracks initiate from the corrosion pit, leading to the fatigue failure below the fatigue limit in laboratory air.

Small Crack Growth Behavior. The relationship between $2c$ and N/N_f in Fig. 5 reveals that cracks initiated at the stage where N/N_f was larger than 0.4 in distilled water, while at an early stage in laboratory air. It

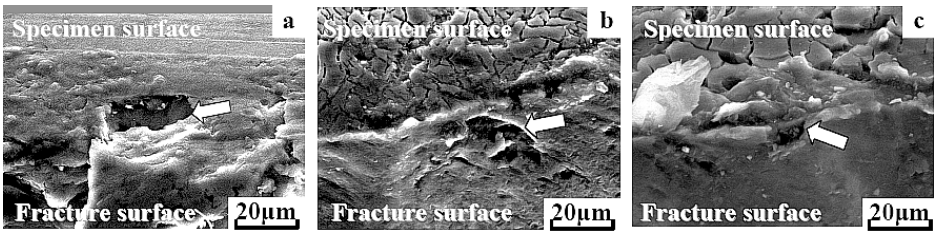

Fig. 7. SEM micrographs showing crack initiation site in distilled water ($\sigma = 50$ MPa): (a) AZ80, (b) AZ61, (c) AM60.

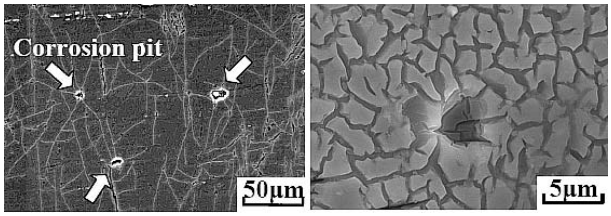

Fig. 8. Specimen surfaces of AM60 ($\sigma = 50$ MPa).

implies that corrosion pits are formed at an early stage of fatigue life in distilled water. Crack growth rates are shown in Fig. 6 as a function of K_{max}. The crack growth rates in distilled water are nearly the same as those in laboratory air, and the dependence of crack growth rate on chemical composition observed in laboratory air disappears in distilled water.

Effect of Chemical Composition. Figure 9 indicates the anode polarization curves in distilled water. The corrosion potentials are almost the same in all alloys, while the corrosion rate is fastest in AZ80. It is believed that the highest sensitivity of AZ80 to corrosive environment is attributed to the electrochemical nature of AZ80. Therefore, it can be concluded that the addition of Al can contribute to improving the fatigue limit in laboratory air, while enhances the sensitivity against corrosive environment. Fatigue behavior in laboratory air and distilled water was similar between AZ61 and AM60, thus the addition of Zn has no effect on fatigue strength and corrosion resistance.

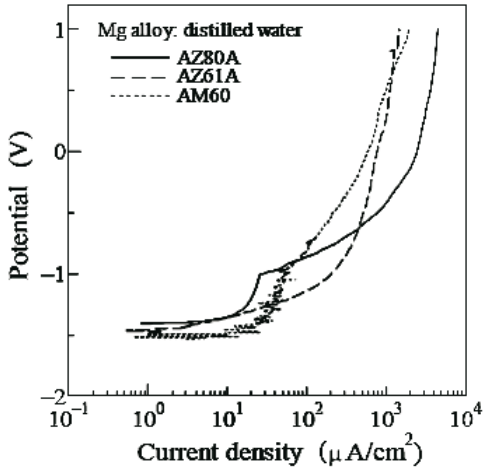

Fig. 9. Anode polarization curves in distilled water.

Conclusions. Rotary bending fatigue tests were conducted in laboratory air and distilled water using three extruded Mg alloys AZ80, AZ61, and AM60 with different chemical compositions. In laboratory air, AZ80 with the largest Al content had the highest fatigue limit, because crack initiation was due to cyclic slip deformation at low stress levels. However, corrosion fatigue strengths were almost the same in all alloys, indicating that the sensitivity against corrosive environment was enhanced by the addition of Al.

REFERENCES

1. Y. Uematsu, K. Tokaji, M. Kamakura, et al., *Mater. Sci. Eng.*, **A434**, 131 (2006).
2. R. S. Stameppa, R. P. M. Procter, and V. Ashworth, *Corrosion Science*, **24**, 325 (1984).
3. Y. Unigovski, A. Eliezer, E. Abramov, et al., *Mater. Sci. Eng.*, **A360**, 132 (2003).